

## COMPARISON OF OPTICAL TRANSITION RADIATION SIMULATIONS AND THEORY

J. Wolfenden<sup>†</sup>, R. Fiorito, C. Welsch, Cockcroft Institute & University of Liverpool, Liverpool, UK  
 T. Lefevre, R. Kieffer, S. Mazzoni, CERN, Geneva, CH  
 P. Karataev, M. Bergamaschi, K. Kruchinin, JAI RHUL, Egham, UK

### Abstract

The majority of optical diagnostics currently used will not stand up to the requirements of the next generation of particle accelerators. Current methodologies need innovation to be able to reach the sub-micrometre resolution and sensitivity that will be required. One technique that has the potential to meet these requirements is optical transition radiation (OTR) imaging. A new algorithm is proposed which incorporates OTR theory, optical effects and beam distribution. This algorithm takes an existing method used for beam imaging and pushes the limits resolution beyond that normally attainable. In doing so, it can provide a reliable and economical diagnostic for future accelerators. A discussion on further applications of the algorithm is also presented.

### INTRODUCTION

In the current generation of particle accelerators optical transition radiation (OTR) is a well-established tool in accelerator beam diagnostics [1, 2, 3]. The resolution of techniques implementing OTR is usually only limited by the resolution of the optics used to capture the radiation. However, as we approach a new generation of accelerators, with emittances and beam sizes hitherto unseen in the current generation, the resolution of OTR methods will begin to be severely restricted by other means.

This is due to the image of OTR captured in measurements is a convolution of the beam distribution, optical effects and the OTR single particle function (SPF) [4]. The SPF is the OTR image one would expect to capture from a single particle. For electron beams, where the OTR is mainly implemented as a diagnostic tool, the width of this SPF is  $\sim \mu\text{m}$ . The limitation in resolution occurs when the beam width approaches the SPF width; the beam distribution is hidden by the SPF and it becomes impossible to directly extract the beam size [5].

In recent years, a new technique has been developed to uncover this hidden beam distribution. The process involves using an empirical function to monitor how the SPF is modified by different beam sizes [5]. This method has been able to achieve resolutions which rival that of more complex techniques such as the laser wire [5].

In conjunction with this technique, optical simulation software Zemax Optical Studio (ZOS) [6] has been used to design an optimum OTR imaging system [7]. It is possible to provide ZOS with a source distribution and have it propagate the transverse electric fields through an optical system which matches an experimental setup. In this way, it is possible to quantify the optical effects associat-

ed with the OTR imaging system, and thus take measures to reduce their effect.

ZOS has previously been used to reproduce the theoretically predicted far-field angular OTR distribution [8]. However, ZOS has never been used to reproduce the field distribution expected in the near field [9], nor has it ever been used to make a comparison with the theoretically predicted OTR SPF [10].

### THEORY BASED ALGORITHM

Filling in these missing pieces provides the tools to produce a new analysis method, which builds upon the previous empirical based method, but also incorporates OTR theory and other well-known effects.

#### Algorithm Structure

The analysis technique is defined by an algorithm which can be separated into three modules, which are presented in Fig. 1. The first component is a theoretical model for the source distribution. For OTR this is well-established [11], and only requires two parameters: the gamma value of the beam,  $\gamma$ , and the wavelength of the OTR,  $\lambda$ .

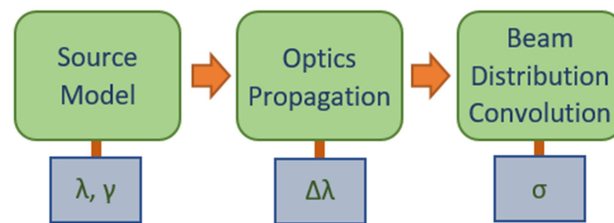


Figure 1: A diagram showing the modular design of the new analysis algorithm. Below each module are the required parameters for that stage.

The second module takes the output of the first module as an input and propagates it through a predefined imaging system model in ZOS. This technique is innovative in that rather than using ZOS as a design tool, it is used as a diagnostic tool. Aside from the model this step requires one other parameter, the bandwidth of the optical system,  $\Delta\lambda$ . In previous methods only single wavelength simulations were used. In reality, all experimental measurements are conducted with a set bandwidth; too small and the intensity of the OTR becomes too weak to detect, too large and the resolution is compromised by the chromatic aberrations of the optical system [12]. This module of the algorithm can produce a convolution of the SPF and a bandwidth function by running the ZOS simulations mul-

multiple times whilst varying the wavelength across the bandwidth. The results of these simulations can then be weighted by the bandwidth filter function and summed together.

The final module of the algorithm takes the output distribution of the second module and convolves this with an estimated beam distribution. This final distribution is matched to measurements by solely varying the beam width,  $\sigma$ .

The algorithm dispenses with the need to use an empirical fit and clarifies the diagnostic dependence of the measured OTR SPF on beam size.

### *Effect of Optics*

Due to the modular design of the algorithm, each calculation is independent of the others. Therefore, the source distribution can be changed without effecting the other modules; equally so for the optical system and the beam distribution.

A consequence of this is that the output of the algorithm,  $\sigma$ , is independent of the optical system. This enables one to isolate and potentially remove all optical effects (e.g. spherical aberrations, chromatic aberrations, etc.) from the measurement, and the associated limitations to the resolution. This greatly reduces the restrictions on any optical imaging system and produces a beam size resolution that can surpass the optical resolution. A caveat must be stated here as although the algorithm can account for aberrations within the optics, the resolution cannot be so poor as to completely obscure the sensitivity of the SPF to beam size.

Another outcome from this modular design is that the source distribution can be any form of radiation, of any wavelength, that can be propagated via optics (e.g. transition radiation, diffraction radiation, synchrotron radiation, etc.). This presents a wide range of potential applications of the algorithm.

## ZEMAX SIMULATION

### *OTR Source Distribution*

The source distribution for OTR is well-defined and understood [11]:

$$E_{x_S, y_S}^S(\vec{r}, \omega) = \frac{e\alpha}{\pi c\beta} \frac{x_S y_S}{\sqrt{x_S^2 + y_S^2}} K_1\left(\alpha\sqrt{x_S^2 + y_S^2}\right), \quad (1)$$

where  $\alpha = \omega/\gamma v$  and  $S$  denotes the source plane. This source distribution can be propagated analytically through an ideal (i.e. thin lens approximation) imaging system to provide the field distribution at the image plane [10]. This distribution could be easily substituted in to replace the output from ZOS. However, the theoretical result for the image lacks the associated effects of the optics; a crucial component needed for the algorithm to be used effectively as a diagnostic tool. This is where ZOS can be applied. It is capable of simulating the various aberrations that can occur in optical systems and the associated loss of resolution. By incorporating these effects into the algorithm, the analysis is able to properly model any experimental setup.

### *ZOS Source Sampling*

To transform Eq. (1) into a ZOS input it is necessary to numerically sample the source plane by way of an input matrix. This process is a balance between the spatial size of the matrix and the sampling resolution across the matrix.

A spatial distance which is large relative to the source size,  $\gamma\lambda$ , needs to be covered by the input matrix [9]. This is because the field properties in the wings of the source distribution contain the information which dictates the position of the central lobes of the OTR SPF. If this region is not sampled correctly then the SPF peak separation will be incorrect. On top of this, there must also be a region of zero-padding surrounding the sampled source distribution. This is a requirement of ZOS to prevent modelling artefacts, but it has the undesired effect of further increasing the size of the input matrix, and subsequently lowers the initial sampling resolution.

With regards to the sampling resolution, this must be high enough to adequately sample the central region of the source distribution, which increases rapidly as  $r_S$  approaches 0. This region contains the near-field information of the source. If this portion of the distribution is insufficiently sampled then the details of the OTR SPF distribution will be incorrect.

These two sampling requirements lead to a situation where a high resolution over a relatively large distance is required to adequately model OTR in ZOS. To avoid the obvious limitations imposed by computational and temporal restrictions, there are several options that can be implemented.

The first is to use a matrix grid with non-constant adaptive sampling. This allows high resolution sampling at the centre of the source, with sufficiently low sampling in the wings to lower the computational strain associated with the simulation. This would be the ideal option, but currently ZOS does not support such functionality [6]. This may however be an option for the future, or with a different simulation tool.

Another sampling option which could be implemented using ZOS is a coordinate transform. A non-constant input matrix grid would be defined, it would then require a coordinate transform to a constant grid; this could then be used as an input to ZOS. Obviously, all output from ZOS would require the reverse transform before any further analysis.

A third option is to analytically calculate the field distribution on a plane at some pre-defined propagation distance, sample at this plane, then input into ZOS. This will have less stringent sampling requirements due to the lack of a singularity at the centre, such as is found in the source distribution. This is the method which has been investigated for this paper and is described below.

### *Intermediate Plane Distribution*

Equation (1) can be propagated using the Fresnel diffraction integral [13], right up to the first surface of the first optic. The result is:

$$E_{x_L, y_L}^L(\vec{r}, \omega) = \frac{-2e\alpha e^{ika} e^{\frac{ikr_L^2}{2a}}}{\lambda\alpha\beta c} \frac{x_L y_L}{\sqrt{x_L^2 + y_L^2}} F_L(a, \alpha, \vec{r}_s), \quad (2)$$

with,

$$F_L(a, \alpha, \vec{r}_s) = \int_0^\infty dr_s K_1(\alpha r_s) J_1\left(\frac{kr_L}{a} r_s\right) e^{\frac{ik}{2a} r_s^2},$$

where  $L$  denotes the plane at first surface of the first optic. This can be used to calculate the OTR field distribution at any propagation distance, assuming there are no apertures or changes in propagation medium.

To ensure that Eq. (2) provided the correct field distribution, it was used to calculate the OTR angular distribution at various multiples of the OTR formation length,  $\gamma^2\lambda$  [9]. These results are presented in Fig. 2, and agree with previous results calculated via a different method [9].

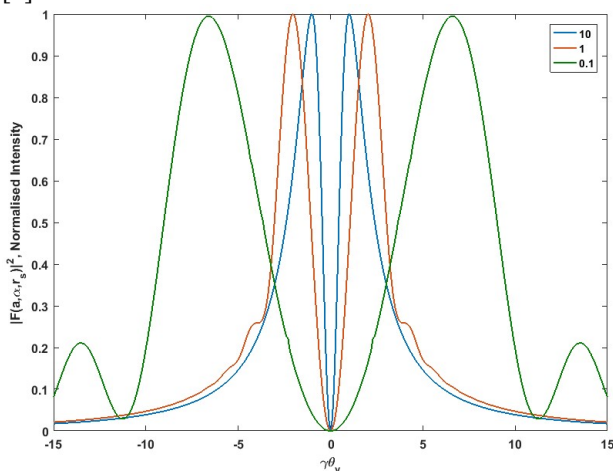


Figure 2: The angular distribution of the OTR intensity for different distances from the source plane. The legend is in units of  $\gamma^2\lambda$ :  $10\gamma^2\lambda$  peaks at  $1/\gamma$ ,  $\gamma^2\lambda$  peaks at  $2.1/\gamma$ ,  $0.1\gamma^2\lambda$  peaks at  $6.6/\gamma$ .

## CONCLUSION

The distributions presented in Fig. 2 validate the result obtained in Eq. (2), but further validation is required. This will begin with simulation of the OTR SPF produced by these intermediate distributions for an ideal imaging system. It will be vital to do this at various distances from the source plane, as Fig. 2 shows, the field distribution of OTR varies dramatically with distance. This work is currently underway.

These simulations will need to be matched to the OTR SPFs predicted by theory. This analytical result can be calculated by propagating Eq. (2) through to an imaging plane [10]. Once this comparison has been achieved, it will then be possible to replace the ideal imaging system in ZOS with that of a real system, with real optics. This is the key draw of ZOS, and an integral part of this new analysis algorithm.

Once these have been achieved, the bandwidth convolution and the beam distribution convolution will be investigated. Neither of these techniques has ever been used in conjunction with theory in a diagnostic setting before.

Another source of potential is the generality of the algorithm. By simply altering the source distribution any optical diagnostic can be analysed. On this note, there are plans to test this analysis outside of the optical range and investigate an application in Terahertz imaging.

## ACKNOWLEDGEMENTS

This work was supported by the EU under Grant Agreement No. 624890 and the STFC Cockcroft Institute core Grant No. ST/G008248/1.

## REFERENCES

- [1] L. Wartski *et al.*, “Interference phenomenon in optical transition radiation and its application to particle beam diagnostics and multiple-scattering measurements”, *J. Appl. Phys.*, vol. 46, p. 3644, Aug. 1975.
- [2] M. Castellano *et al.*, “Analysis of optical transition radiation emitted by a 1 MeV electron beam and its possible use as diagnostic tool”, *Nucl. Instr. Meth. Phys. Res. Sect. A*, vol. 357, p. 231-237, 1995.
- [3] C. Thomas, N. Delerue, and R. Bartolini, “Single shot transverse emittance measurement from OTR screens in a drift transport section”, *J. Instr.*, vol. 6, p. 07004, 2011.
- [4] D. Xiang and W.-H. Huang, “Theoretical considerations on imaging of micron size electron beam with optical transition radiation”, *Nucl. Instr. Meth. A*, vol. 570, p. 357-364, 2007.
- [5] K. Kruchinin *et al.*, “Sub-micrometer transverse beam size diagnostics using optical transition radiation”, *J. Phys.: Conf. Series*, vol. 517, p. 012011, 2014.
- [6] Zemax 16.5 SP4, Optical Design Program, User’s Manual, (2017).
- [7] B. Bolzon *et al.*, “Very high resolution optical transition radiation imaging system: Comparison between simulation and experiment”, *Phys. Rev. ST Accel. Beams*, vol. 18, p. 082803, Aug. 2015.
- [8] T. Aumeyr *et al.*, “Advanced simulations of optical transition and diffraction radiation”, *Phys. Rev. ST Accel. Beams*, vol. 18, p. 042801, Apr. 2015.
- [9] V. A. Verzilov, “Transition radiation in the pre-wave zone”, *Phys. Lett. A*, vol. 273, p. 135-140, Aug. 2000.
- [10] L. G. Sukhikh, G. Kube, A. P. Potylitsyn, “Simulation of transition radiation based beam imaging from tilted targets”, *Phys. Rev. Accel. Beams*, vol. 20, p. 032802, Mar. 2017.
- [11] M. L. Ter-Mikaelian, *High-Energy Electromagnetic Processes in Condensed Media*, New York, Wiley Interscience, 1972.
- [12] J. Wolfenden *et al.*, “Optical effects in high resolution and high dynamic range beam imaging systems”, in *Proc. Int. Beam Instr. Conf. (IBIC’16)*, Barcelona, Spain, Sep. 2016, paper WEPG80, p. 844-847.
- [13] M. Born, E. Wolf, *Principles of Optics*, 5th Ed., Oxford, Pergamon Press, 1975.